Proceedings of the World Congress on Engineering 2022
WCE 2022, July 6 - 8, 2022, London, U.K.

Regularized Artificial Neural Networks for Predicting the Strain of Traction-Aged Polymer Systems Part II

Helene Canot, Philippe Durand, Emmanuel Frenod, Bouchera.Hassoune-Rhabbour, Valerie.Nassiet

***Abstract*—In this paper, we study the aging factor of a new polymer B and second time on A-150, A-185 polymer systems already certified for use in the aircraft and aerospace industry and we formulate a predictive model of sustainability thanks to artificial neural networks. It is the continuation of the paper [] in which we approach the experimental problem and the the theoretical part concerning Bayesian regularization and the BFGS algorithm. In this paper, an initial small experimental dataset of 33 samples is used to analyze the strain of polymers systems as a function of aging time, temperature, Young modulus and the breaking stress. In the view of the very small dataset, the strain of polymers systems is predicted by training Levenberg–Marquardt (LM), Bayesian regularization (BR), and Broyden-Fletcher-Goldfarb-Shanno (BFGS) algorithm with a regularized cost function algorithms. The best results have been obtained with the two regularized artificial neural network from very small data set.**

***Index Terms*—rtificial Neural Network Multi-Layer Perceptron Bayesian Regularization Levenberg Marquardt and BFGS Polymer system Lifetimertificial Neural Network Multi-Layer Perceptron Bayesian Regularization Levenberg Marquardt and BFGS Polymer system LifetimeA**

I. Introduction

In our article we are interested in the characterization of polymer systems aged in traction resulting from the experimental study at the LGP (Laboratoire Génie de Production) of Tarbes. In particular, the data from this study, for polymer B, will serve as a basis for training an Artificial Neural Network (ANN). In the first part, we introduced the experimental problem and we approached the regularization methods for the ANNs that we used.

The objective is therefore to find a compromise between the quality of learning and the capacity for generalization. Also first, we evaluate training performance of the Levenberg-Marquardt(LM) algorithm without regularization, compared with two regularization algorithms. This part presents the results of the different stages of the modeling: a phase of calculation carried out in order to determine the architecture of the optimal ANN and its validation before moving on to predictions. Secondly, regularized ANN were employed to predict strain of the polymer B and thirdly the polymers A-150, A-185.

Helene Canot is in Université de Bretagne-Sud, UMR 6205, LMBA, F-56000 Vannes, France e-mail:helene.canot@univ-ubs.fr,
Philippe Durand is in M2N, Conservatoire National des Arts et Métiers, 292 rue Saint Martin, 75141 Paris FRANCE e-mail:philippe.durand@lecnam.net,
Emmanuel Freod is in Université de Bretagne-Sud, UMR 6205, LMBA, F-56000 Vannes, France e-mail:emmanuel.frenod@univ-ubs.fr,
Valerie Nassiet and Bouchera.Hassoune-Rhabbour are in: ENIT, 47, avenue d'Azereix - BP 1629 - 65016 Tarbes CEDEX, France, Equipe IMF, France, e-mail:valerie.nassiet@enit.fr, bouchra.hassoune-rhabbour@enit.fr

This paper is organized as follows: section II presents the results and discussion in section III we concluded the part I and the part II of the papers.

II. Results and Discussions

A. Implemention of ANN

We trained the LM, BR and BFGS networks, multiple times with 33 vectors by changing the number of hidden layer neurons and selected the one which gave best results for prediction. For the Bayesian Regularization Artificial Neural Network (BRANN), the regularization parameters (β, α) were optimized following(Part I, III-B) . The validation set is not essentially required in the case of the regularization methods.

To evaluate the performance of the three networks, mean squared error (MSE) and correlation coefficient R are estimated. The MSE measures the deviation between original values and predicted ones, and R provides information on the strength of correlation between them. They are defined by the equations below:

$$MSE = \frac{1}{N}\sum_{i=1}^{N}(y_i - y_i')^2 \tag{1}$$

$$R = \frac{\sum_{i=1}^{N}(y_i-\overline{y})(y_i'-\overline{y'})}{\sqrt{\sum_{i=1}^{N}(y_i-\overline{y})^2 \ \sum_{i=1}^{N}(y_i'-\overline{y'})^2}} \tag{2}$$

where y_i is the observed value and y_i' is the network output value. y' and $\overline{y'}$ are respectively the average of the real value and the network output value, and N is the sample number. The MSE and the number of neurons in the hidden layer are investigated to construct the optimal structure of the neural network.

The MSE depending on iteration (epochs) of the BRANN is shown in the Figures above. In red, the error on the test set, in green the error on the validation set. In blue, the learning error. If the validation and test error increase while the training error continues to decrease then there is overfitting. The training stopped when the MSE value was achieve. A negligible value of the MSE indicates the high degree of correlation among input variables. Training stops when any of these conditions occurs: 1) the maximum number of epochs is reached, 2) performance of the network with the number of neurons has met a suitable level, 3) performance is minimized to the goal 4) the gradient was below a suitable target 5) μ exceeds $\mu_{max} = 10^{10}$. In conclusion, we see the effectiveness of the regularization methods. Indeed, we clearly observe in the left figure 2 of the supervised training performance an overfitting.

ISBN: 978-988-14049-3-0
ISSN: 2078-0958 (Print); ISSN: 2078-0966 (Online)

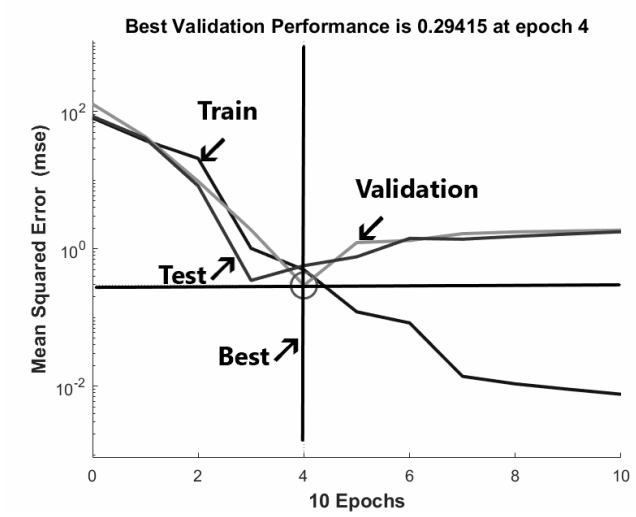

Fig. 1. Performance of the feedforward neural network without regularization

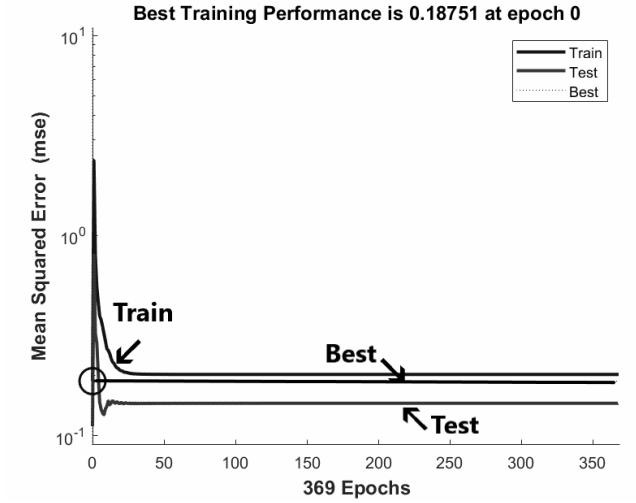

Fig. 2. Performance of the Bayesian neural network

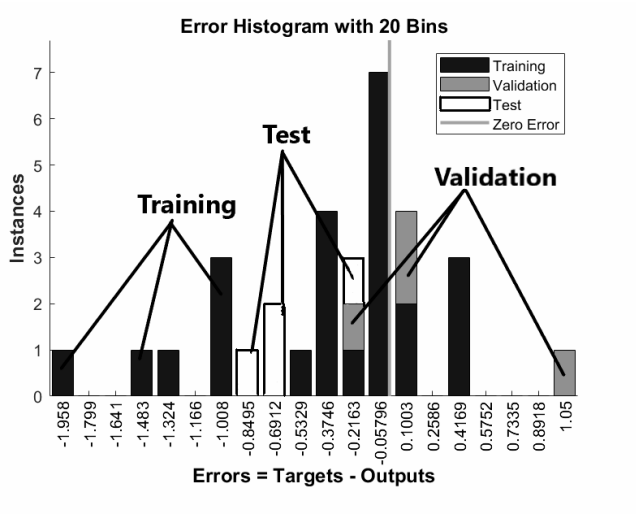

Fig. 3. Error histogram for Neural network without regularisation

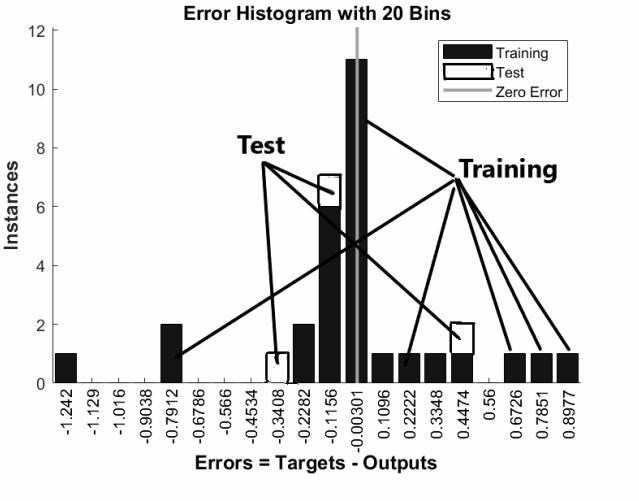

Fig. 4. Error histogram for the Bayesian regularization neural network

The two figures of histograms represent the errors between target values and predicted values after training ANN. These error values indicates how predicted values are differing from the target values. Y-axis represents the number of samples from dataset, which lies in a particular bin. For example for the BRANN, we have a bin corresponding to the error of -0.0031 and the height of that bin for training dataset lies near to 11, the height of bar in the bar plot means how many data points are near the bin value. It means that 11 samples from training dataset have an error lies in the following range. Zero error line corresponds to the zero error value on the X-axis. We can see on the left histogram that the errors are much more dispersed: the difference is between -1.95 and 1.05, the majority of errors correspond to 7 samples with an error of -0.057.

The the regression coefficient figures show a better performance of R for the BRANN with regularization whose R is close to 0.95 against 0.92 for the NN without regularization. For the BRANN, the outputs are correlated with the corresponding target values for training and testing, the R value is 0.9599 for the total response. There is a relatively linear relationship between outputs and targets. These results show a good fit at the level of training and testing. It was shown that there is a good correlation between the predicted values

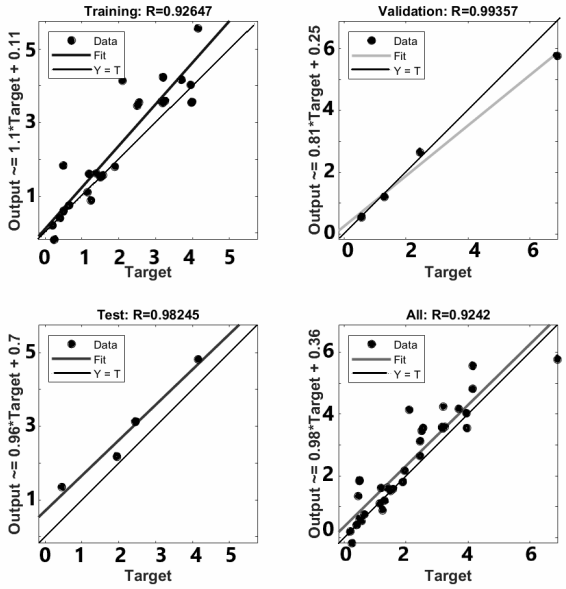

Fig. 5. Regression of the neural network without regularization

of BRANN and the experimental values. After several tests

ISBN: 978-988-14049-3-0
ISSN: 2078-0958 (Print); ISSN: 2078-0966 (Online)

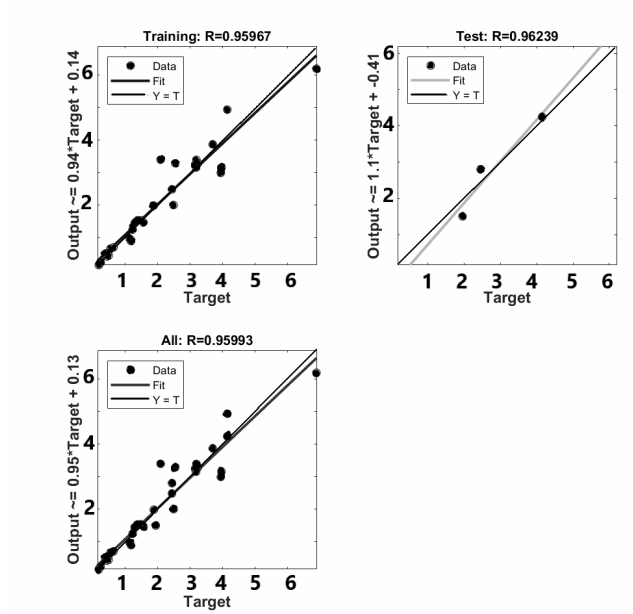

Fig. 6. Regression of Bayesian regularization neural network

the optimal neural architecture is composed of 12 neurons with the performance equal to 0.1857.

Now the optima structure and the performance parameters of the three networks are summerized Table I.

TABLE I
MEAN SQUARED ERROR AND EPOCHS FOR DIFFERENT ARCHITECTURES.

Network models	Network structures	MSE	Epochs
LM	4 - 5 - 1	0.4642	8
BFGS	4 - 12 - 1	0.1861	300
BR	4 - 12 - 1	0.1803	369

The models training is performed with 4 to 15 hidden neurons. By increasing the neural network structure of one neuron each time and comparing the mean square error, it attains a minimum for the BRANN model with 12 neurons. The minimum values are obtained for the two regularized models. So, the model can be explained well with small data set when Bayesian Regularization is used for training the networks. Once the BRANN model has learned well, it interpolates the data according to an implicit function of the following form:

$$\varepsilon = f(t, T, E, \sigma) \tag{3}$$

B. ANN prediction results for the polymer B.

Now, we are going to make all of our predictions in our work with the BR and BFGS algorithms.

In this section, first we trained the models with a dataset containing 32 samples (at 33 samples we remove the last value for aging time t=15th month for $T = 70°C$) of the polymer B. After having selected for each model the optimal structure we predicted the following value for $T = 70°C$ and aging time t = 15th month.

In order to verify the ability of the models to predict data outside the database, some following data for aging time t=15 months. The prediction results and the statistical parameters are presented in Table II. It can be seen that the regularized models have good performance. This means that the regularized models have a good ability to predict the unknown data and a better performance compared to the unregulated model.

TABLE II
STATISTICAL PARAMETERS OF THE PREDICTED STRAIN OF THE POLYMER B FOR $T = 70°C$, T=15 MONTHS.

Network models	$\varepsilon(\%)$	predicted $\varepsilon(\%)$	MSE
BFGS	1.45	1.38	0.0043
BR	1.45	1.51	0.0036

According to the performance calculations for the strain prediction for $T = 70°C$, and aging time t=15 months, Bayesian regularization gives the best result with a mean square error of 0.0036 against 0.0043 for BFGS.

Secondly, a case with even smaller subset of the data was considered with 28 samples (at 33 samples we remove the last five samples for aging time 3th, 6th, 9th, 12th and 15th months for $T = 70°C$) and we predicted strain values for aging time the 3th, 6th, 9th, 12th and 15th months and $T = 70°C$.

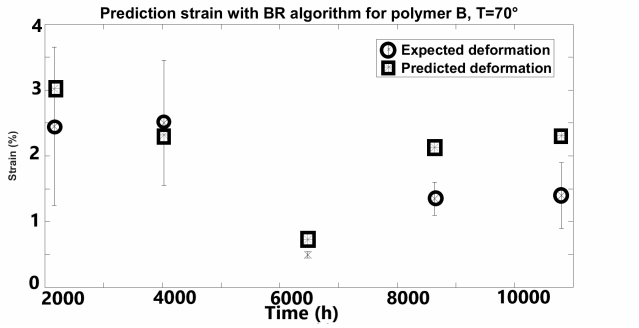

Fig. 7. Prediction by the BR algorithm of the deformation of the polymer B, for the last five terms of the experiment

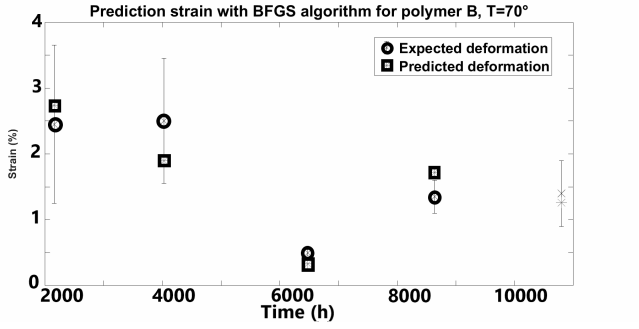

Fig. 8. Prediction by the BFGS algorithm of the deformation of the polymer B, for the last five terms of the experiment

As shown in Fig. 8, with the BFGS algorithm, the last five values predicted of strain are close to the desired outputs results, in particular within the interval of uncertainties. These results show that the BFGS regularization is accurate even with a small dataset. However, for BRANN the predicted strain values show deviation from the desired target result and three points do not belong to the uncertainty interval. The MSE corresponding are given Table III and it confirms

ISBN: 978-988-14049-3-0
ISSN: 2078-0958 (Print); ISSN: 2078-0966 (Online)

that the performance of BRANN is a little worse than that of BFGS:

TABLE III
PREDICTION OF THE STRAIN OF THE POLYMER B FOR $T = 70°C$, AND AGING TIME T= 3, 6, 9, 12 AND 15 MONTHS.

Network models	MSE
BFGS	0.108
BR	0.356

From the cases, we observed that the predictions of BRANN model are closer to the experimental target values even with a small training data set. But in the last case where a prediction of the strain is requested for many aging times t=3, 6, 9, 12 and 15 months, BFGS performs better than BR. The accuracy of the regularized models decrease when increasing the number of points to predict. Both regularized algorithms are able to predict, despite a small data set, for aging times depending on the mechanical characteristics of a polymer. This means that during experimental work a neural network is able to predict for the next three, six, nine months.

This type of prediction, with a quality of precision even for small datasets which is often the case in the field of materials, can make it possible to continue and complete experiments. It allows to reduce the time and the cost in long experiments, for the study of the durability of polymers. Monitoring the aging of polymers over several months is costly and restrictive. ANNs can be an effective tool, even on small samples, to test the behavior and performance of materials.

C. Prediction of the strain for the polymers A-150 and A-185.

Now, an already trained neural network is used to make predictions on new data with variables that have been generated by the same underlying processes and relationships as the original dataset that was used to train the model. The possibility of generalization is an essential characteristic of neural networks. We tested Bayesian methods and regularized BFGS methods on other polymer systems at the same conditions that the system B. We explore characterization of polymer systems aged in traction on systems A-185 and A-150. The entire sample of polymer B was used to train the neural network. Time aging, temperature, elasticity modulus and stress was used as inputs contained 33 experimental data and the strain as output. Then, the trained neural network on polymer B was requested to predict the points of the strain for $T = 70°C$ of polymers A - 150, A- 185. A comparison is then made between the forecast values obtained with the experimental data. Figures 9, 10, 11 and 12 below next illustrate this comparison. The red point represents the expected results according to the network formed and the blue point represents the experimental results.

The table below gives MSE corresponding of the prediction of the ANNs on these polymer systems.

A perfect match between the experimental values and the predicted values of the polymers A was not expected. According to the results of Table IV, the performance of the network are a little worse than the prediction on polymer B, with however a larger number of points to be predicted. We note, on the one hand, that the BFGS algorithm gives better results than BR for the two polymers A. On the other hand, predictions are better for the long times and much more accurate than on short times. Here we therefore reach the limits of the neural network training on a small set of

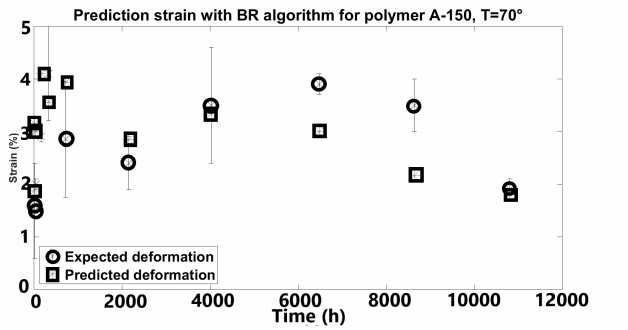

Fig. 9. The comparison of experimental and predicted strain for polymer A-150 with Bayesian regularization

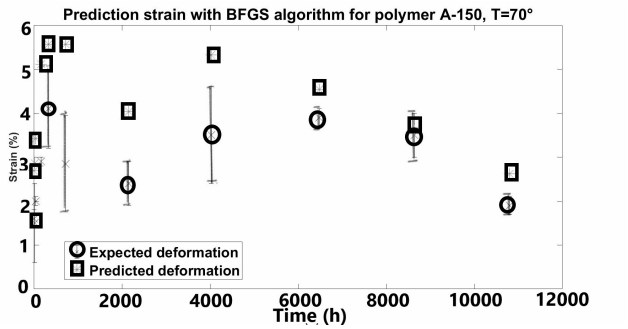

Fig. 10. The comparison of experimental and predicted strain for polymer A-150 with BFGS algorithm

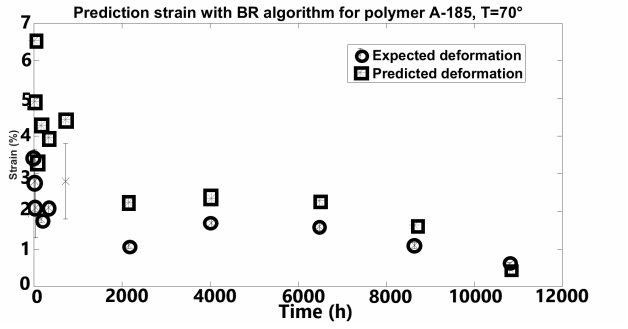

Fig. 11. The comparison of experimental and predicted strain for polymer A-185 with Bayesian regularization

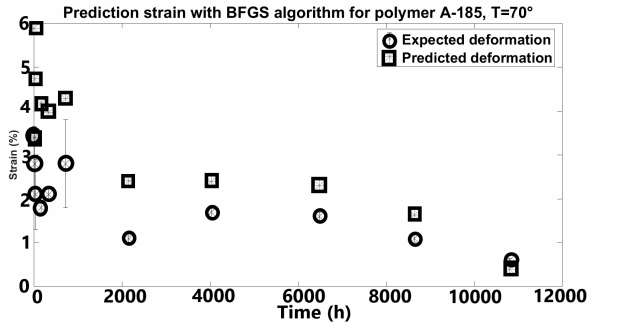

Fig. 12. The comparison of experimental and predicted strain for polymer A-185 with BFGS algorithm

ISBN: 978-988-14049-3-0
ISSN: 2078-0958 (Print); ISSN: 2078-0966 (Online)

TABLE IV
PREDICTION OF THE STRAIN FOR $T = 70°C$ OF THE POLYMERS A-150 AND A-185.

Network models	MSE (A-185 $70°C$)	MSE (A-150 $70°C$)
BFGS	2.35	0.86
BR	2.4	2.45

data. However, we note that the predicted strains have the same tendency as the experimental strains.

III. CONCLUSION

In with work, Bayesian Regularization and BFGS with modified performance function models are employed to predict the strain of traction-aged polymer systems. In the first stage, regularized ANN and ANN model without regularization were built using a very small dataset of 33 samples. The training phase of the ANNs is performed taking into consideration several parameters, such as the aging time, temperature, tensile stress and Young's modulus. The optimal architecture model which contains a sigmoid function and an output layer which contains a linear function, is evaluated using mean square error (MSE) and the regression value R. It is concluded that the Bayesian regularization training algorithm and BFGS regularized algorithm show better performance than the Levenberg–Marquardt algorithm without regularisation. Regularized algorithm can solve the overfitting problem which is not the case of Levenberg–Marquardt algorithm for a small data set.

In a second stage, regularized ANN models, with three datasets of 32, 30 and 28 samples, are used to predict the percent strain of the system B for several aging times. BRANN showed higher performance for one aging time, three aging times predictions. Finally in a third stage, these regularization methods are also used for two different polymer systems : the polymers A-150 and A-185 that were not in the training dataset. Considering the limitations of the model, due to the small dataset, the neural network can more accurately predict the results of the two polymers for long times than for short times. However, the network successfully predicted the strain trend for both polymers.

This allows us to conclude that these two regularized ANN are reliable despite small data. These ANN approaches can be used to predict the trend for the next few months, which saves time and cost in the experimental field.

REFERENCES

[1] OT. Adesina, T. Jamiru, I. Daniyan, R. Sadiku, O. Ogunbiyi, O. Adesina, LW.Beneke (2020). Mechanical property prediction of SPS processed GNP/PLA polymer nanocomposite using artificial neural network. Cogent Engineering. 7. 10.1080/23311916.2020.1720894.

[2] E. Arzaghi, MM. Abaei, R. Abbassi, V. Garaniya, C. Chin, F. Khan (2017) Riskbased maintenance planning of subsea pipelines through fatigue crack growth monitoring. Eng Fail Anal 79:928–939.

[3] L. Barbosa, G. Gomes, A. Ancelotti. (2019). Prediction of temperature-frequency-dependent mechanical properties of composites based on thermoplastic liquid resin reinforced with carbon fibers using artificial neural networks. The International Journal of Advanced Manufacturing Technology. 105. 1-14. 10.1007/s00170-019-04486-4.

[4] H E. Balcıoglu, A. Agdas Seckin and M. Aktas. (2016) Failure load prediction of adhesively bonded pultruded composites using artificial neural network. Journal of Composite Materials 2016, Vol. 50(23) 3267–3281. DOI: 10.1177/0021998315617998

[5] E. Burgaz, M. Yazici, M. Kapusuz, S. H. Alizir, H. Özcan. (2014). Prediction of thermal stability, crystallinity and thermomechanical properties of poly (ethylene oxide)/clay nanocomposites with artificial neural networks. Thermochimica Acta. 575. 159–166. 10.1016/j.tca.2013.10.032.

[6] D. Colombini, J.J. Martinez-Vega, and G. Merle. (2002) Dynamic mechanical investigations of the effects of water sorption and physical ageing on an epoxy resin system. Polymer, 43(16):4479-4485.

[7] A.Doblies, B. Boll, and B. Fiedler. (2019) Prediction of Thermal Exposure and Mechanical Behavior of Epoxy Resin Using Artificial Neural Networks and Fourier Transform Infrared Spectroscopy.Polymers (Basel). Feb; 11(2): 363.

[8] T. Dyakonov, P.J. Mann, Y. Chen, and W.T.K. Stevenson. (1996) Thermal analysis of some aromatic amine cured model epoxy resin systems. II: Residues of degradation. Polymer Degradation and Stability, 54(1):67-83.

[9] B.C. Ennis, P.J. Pearce, and C.E.M. Morris. (1989) Aging and performance of structural film adhesives. III. Effect of humidity on a modern aerospace adhesive. Journal of Applied Polymer Science, 37(1):15-32.

[10] F. Dan. Foresee and Martin T. Hagan. (1997) Gauss-Newton approximation to Bayesian learning. Proceedings of the International Joint Conference on Neural Networks, June.

[11] L. Gavard, Hkdh Bhadeshia, D. J. C. MacKay, and S. Suzuki. (1996) Bayesian neural network model for austenite formation in steels. Materials Science and Technology, 12(6):453–463.

[12] ATC. Goh. (1995) Back-propagation neural networks for modeling complex systems. Artificial Intelligence in Engineering 9:143–15.

[13] N. Huber, Ch. Tsakmakis, (2001). A neural network tool for identifying the material parameters of a finite deformation viscoplasticity model with static recovery. Computer Methods in Applied Mechanics and Engineering 191, 353–384.

[14] Z. Zhang, P. Klein, and K. Friedrich. (2002) Dynamic mechanical properties of ptfe based short carbon fibre reinforced composites: experiment and artificial neural network prediction. Composites Science and Technology, 62(7-8):1001–1009.

[15] S. Koroglu, P. Sergeant, and N. Umurkan. Comparison of analytical, Finite element and neural network methods to study magnetic shielding. Simul. Model. Pract. Theory, 18(2):206216, 2010. doi:10.1016/j.simpat.2009.10.007.

[16] N. Kiuna, C.J. Lawrence, Q.P.V. Fontana, P.D. Lee, T. Selerland, P.D.M. Spelt. A model for resin viscosity during cure in the resin transfer moulding. process. Composites : Part A (33):1497-1503, 2002.

[17] M. Lefik and B.A. Schreer. (2003) Artificial neural network as an incremental non-linear constitutive model for a finite element code. Comput. Methods Appl. Mech. Eng., 192(28-30):32653283, 2003. doi:10.1016/S0045-7825(03)00350-5.

[18] S.Mahmoudi. (2017) Dynamique des structures composites linéaire et non-linéaire en présence d'endommagement. (Doctorial thesis). Université de Bourgogne Franche-Comté.

[19] https://www.mathworks.com/help/nnet/ref/trainbr.html

[20] W. S. McCulloch W. Pitts. (1943) A logical calculus of the ideas immanent in nervous activity. The Bulletin of Mathematical Biophysics, vol. 5, no. 4, pages 115–133.

[21] D.J.C. Mackay. (1992) Bayesian interpolation. Neural Comput. 4, 415–447.

[22] I. Merdas, F. Thominette, A. Tcharkhtchi, and J. Verdu. (2002) Factors governing water absorption by composite matrices. Composites Science and Technology, 62(4):487-492.

[23] D. W. Marquardt,(1963), An algorithm for least-squares estimation of non-linear parameters. Journal of the society for Industrial and Applied Mathematics, 11(2), 431- 441.

[24] M. Minsky S. P. Perceptrons. (1969). An Introduction to Computational Geometry Cambridge Ma.

[25] L. Qingbin, J. Zhong, L. Mabao, W. Schichum, (1996). Acquiring the constitutive relationship for a thermal viscoplastic material using an artificial neural network. Journal of Materials Processing Technology 62, 206–210.

[26] Y. Pei, K. Wang, M. Zhan, W. Xub, X. Ding. Thermal-oxidative aging of DGEBA/EPN/LMPA epoxy system : Chemical structure and thermalemechanical properties. Polymer Degradation and Stability, 96:1179-1186, 2011.

[27] S. Popineau, C. Rondeau-Mouro, C. Sulpice-Gaillet, and M.E.R. Shanahan. (2005) Free/bound water absorption in an epoxy adhesive. Polymer, 46(24):10733-10740.

[28] L.Poussines. (2012) Développement de nouveaux matériaux pour l'infusion de composites.(Doctorial thesis). ENIT Tarbes.

[29] S. Pruksawana, G. Lambard, S. Samitsu, K. Sodeyama and M. Naitoa. Prediction and optimization of epoxy adhesive strength from a small dataset through active learning. Science and Technology of Advanced Materials 2019, Vol. 20, N°. 1, 1010–1021 https://doi.org/10.1080/14686996.2019.1673670

ISBN: 978-988-14049-3-0
ISSN: 2078-0958 (Print); ISSN: 2078-0966 (Online)

[30] F. Rosenblatt. (1962) Principles of neurodynamics.
[31] S. B. Singh, Hkdh Bhadeshia, D. J. C. MacKay, H. Carey, and I. Martin. (1998) Neural network analysis of steel plate processing. Ironmaking Steelmaking, 25(5):355–365.
[32] D.C. Souza, (2015) Neural Network Learning by the Levenberg–Marquardt Algorithm with Bayesian Regularization. Available online: http://crsouza.blogspot.com/feeds/posts/default/webcite.
[33] G.Z. Xiao and M.E.R. Shanahan. (1998) Swelling of DGEBA/DDA epoxy resin during hygrothermal ageing. Polymer, 39(14):3253-3260.
[34] J. Verdu. (2000) Action de l'eau sur les plastiques. Techniques de l'ingénieur, p.1-8.
[35] M. Wiciak-Pikuła, A. Felusiak-Czyryca and P. Twardowski (2020) Tool Wear Prediction Based on Artificial Neural Network during Aluminum Matrix Composite Milling. MDPI. Proceedings of the 2020 IEEE International Workshop on Metrology for AeroSpace, Pisa, Italy, 22–24 June 2020.
[36] Zhang, Zhong Friedrich, Klaus. (2003). Artificial Neural Networks Applied to Polymer Composites: A Review. Composites Science and Technology - Composites SCI Technol. 63. 2029-2044. 10.1016/S0266-3538(03)00106-4.

ISBN: 978-988-14049-3-0
ISSN: 2078-0958 (Print); ISSN: 2078-0966 (Online)